Available online at www.sciencedirect.com
ScienceDirect
Ceramics International 34 (2008) 625–629
CERAMICS INTERNATIONAL
www.elsevier.com/locate/ceramint

Infiltration of Al_2O_3/Y_2O_3 mix into SiC ceramic preforms

S.P. Taguchi *, S. Ribeiro, R.M. Balestra

Escola de Engenharia de Lorena (EEL), Universidade de São Paulo (USP), Polo Urbo Industrial, Gleba AI-6, s/n, CP 116-12600-970 Lorena, SP, Brazil

Received 14 August 2006; received in revised form 20 October 2006; accepted 5 January 2007
Available online 31 January 2007

Abstract

Silicon carbide ceramics are very interesting materials to engineering applications because of their properties. These ceramics are produced by liquid phase sintering (LPS), where elevated temperature and time are necessary, and generally form volatile products that promote defects and damage their mechanical properties. In this work was studied the infiltration process to produce SiC ceramics, using shorter time and temperature than LPS, thereby reducing the undesirable chemical reactions. SiC powder was pressed at 300 MPa and pre-sintered at 1550 °C for 30 min. Unidirectional and spontaneous infiltration of this preform by Al_2O_3/Y_2O_3 liquid was done at 1850 °C for 5, 10, 30 and 60 min. The kinetics of infiltration was studied, and the infiltration equilibrium happened when the liquid infiltrated 12 mm into perform. The microstructures show grains of the SiC surrounded by infiltrated additives. The hardness and fracture toughness are similar to conventional SiC ceramics obtained by LPS.

Keywords: B. Microstructure-final; C. Mechanical properties; D. SiC

1. Introduction

It is well known that the bonds between silicon and carbon atoms in SiC (silicon carbide) are very strong. As a consequence, SiC has a low self-diffusion coefficient. This property limits the production of high density SiC ceramics without additive. In order to get a high density ceramic, some metallic oxides (additives) can be added to SiC in liquid phase sintering (LPS), which results in a material with an homogeneous microstructure and therefore suitable to achieve good mechanical properties, such as a high toughness and hardness, 3–5 MPa $m^{1/2}$ and 15–20 HV, respectively [1–4].

The mix SiC plus additive can be produced by infiltration process. This process has grown to become one of the most significant methods of composite production, mainly ceramic–metal composites. There are many works on ceramic–metal materials obtained by infiltration but there are only few works on ceramic-ceramic. The spontaneous process of infiltration is very attractive because in this process external pressure is not used, and it is more economical than the process in which external pressure is used [5–15].

The capillarity pressure is driving force of the spontaneous infiltration of the liquid into packed particulate preforms, and depends strongly on the shape and size of the interconnected pores, and wettability between liquid and solid of the preforms. The wettability between Al_2O_3/Y_2O_3 and SiC is very good [16]. Theoretical treatments are based on the assumption that pores are a bundle of parallel capillaries forming a complex pore structure in the preforms. It makes very difficult to apply simple capillarity rise and viscous flow equations to infiltration, but some experimental results illustrated that the infiltration kinetics depends on the viscosity and density of the liquid [11,14,15]. Usually, the kinetics infiltration curve (infiltration height versus time) presents exponential behavior [17–19].

The objective of this work was to study the infiltration behavior of Al_2O_3/Y_2O_3 mix in SiC, aiming the SiC ceramic production at temperature and times smaller than in liquid phase sintering.

2. Experimental

The β-SiC powder (H.C. Starck, type BF-12) was pressed at 30 MPa in the disks shape of 10 mm diameter and pressed isostatically at 300 MPa. The SiC preforms were pre-sintered in argon atmosphere, at 1550 °C for 30 min. These preforms were machined to the dimension of Fig. 1(a). This shape was used to

---

* Corresponding author. Tel.: +55 12 3159 9900; fax: +55 12 3153 3006.
E-mail address: simone@demar.eel.usp.br (S.P. Taguchi).

0272-8842/$34.00 © 2007 Elsevier Ltd and Techna Group S.r.l. All rights reserved.
doi:10.1016/j.ceramint.2007.01.001

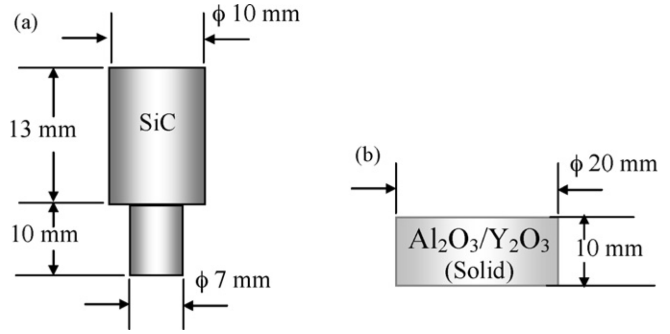

Fig. 1. Schemes of: (a) SiC perform and (b) Al_2O_3/Y_2O_3 disc used in the infiltration tests.

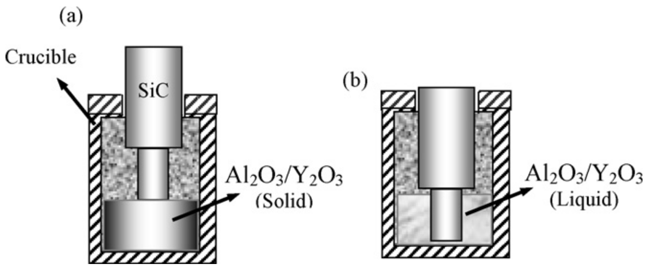

Fig. 2. Schemes of SiC/Al_2O_3/Y_2O_3/crucible used in the infiltration tests: (a) before Al_2O_3/Y_2O_3 melting and (b) after Al_2O_3/Y_2O_3 melting.

the ‘‘indirect infiltration’’ that describes the unidirectional infiltration.

The Al_2O_3/Y_2O_3 mix, with 64.35 wt.% of Al_2O_3 and 35.65 wt.% of Y_2O_3 was mixed in an attrition mill for 1 h, at 1000 rpm, in pure isopropyl alcohol, and dried at 80 °C. The Al_2O_3/Y_2O_3 mix were pressed at 30 MPa, Fig. 1(b), and sintered at 1500 °C for 1 h in air atmosphere.

The SiC preforms and Al_2O_3/Y_2O_3 discs of each infiltration test were placed in a graphite crucible, as shown in Fig. 2(a), and they were heated in argon atmosphere, at 1870 °C for 5, 10, 30 and 60 min. This temperature was chosen on the basis of the wettability test results, made by Taguchi et al. [16]. This temperature is approximately 100 °C above the melting point, where the Al_2O_3/Y_2O_3 discs were completely melted, Fig. 2(b), in which the contact angle presented lowest value. After heating the samples were cooled at a rate of 40 °C/min. The mass quantities of Al_2O_3/Y_2O_3 were enough to infiltrate completely all preforms, but the Al_2O_3/Y_2O_3 liquid did not touch the unidirectional section of the SiC during the test. The submerged section was not analyzed.

After infiltration, the samples were cut longitudinally, ground and polished up to 1 μm of diamond suspension. The infiltration advances in the samples were analyzed using a scanning electron microscope (SEM) with energy dispersive spectrometer (EDS), mapping the elemental composition on the

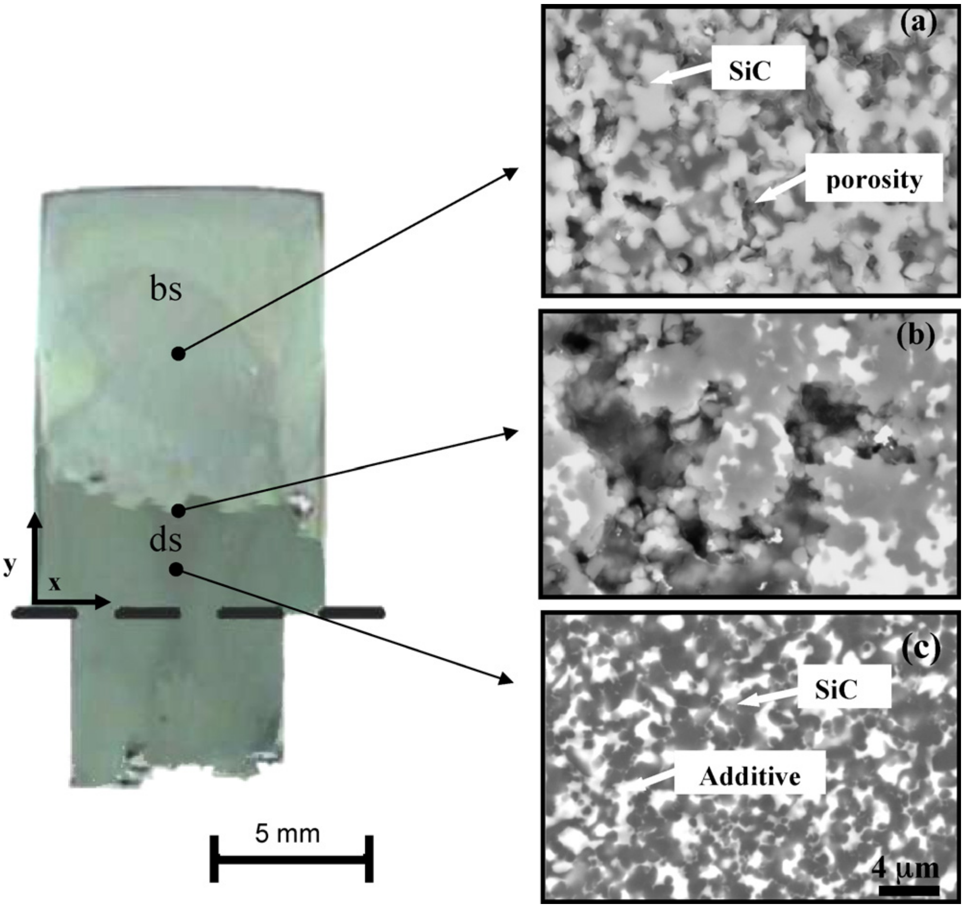

Fig. 3. SiC preform infiltrated with Al_2O_3/Y_2O_3 at 1870 °C for 5 min (at left), when the x and y axes determine the directions of the EDS point-mapping. Microstructures obtained by SEM in backscattering mode (at right), of (a) SiC non-infiltrated region, (b) SiC/infiltrated interface and (c) infiltrated region.

infiltrated cross sections of the samples. The analysis used a LEO1450VP SEM with Oxford INCA Energy EDS system.

The Vickers hardness (H_v) of infiltrated region of sample was analyzed using a Micromet 2004-BUEHLER machine, at 20 kN load and 30 s loading time. The fracture toughness (K_{IC}) was measured by indentation crack length (ICL) method using Antis et al. equation [20], Eq. (1):

$$K_{IC} = 0.016\left(\frac{E}{H_v}\right)^{0.5} P(c)^{-3/2} \quad (1)$$

where E is Young modulus, P is the force and c is the length of crack obtained after indentation.

3. Results and discussion

The driving force for the spontaneous infiltration of the liquid into packed particulate preforms is the capillarity pressure that depends strongly on the shape and size of the interconnected pores and wettability between liquid and solid phases of the preform. The behavior of the liquid on the solid surface is generally indicated by the contact angle θ, which is expressed as a function of the surface energies [4,16]. The work about wettability of SiC by Al_2O_3/Y_2O_3 liquid, made by Taguchi et al. [16], showed contact angle around 4° at 1870 °C. At this temperature, Al_2O_3/Y_2O_3 had completely melted and the wetting of system is enough to enable spontaneous infiltration to take place, because the contact angle is smaller than the critical contact angle ($\theta < 90°$).

Fig. 3 (at left) shows the photo of SiC preforms infiltrated with Al_2O_3/Y_2O_3 at 1870 °C for 5 min, when the x and y axes indicate the directions of the EDS point-mapping. This mapping show the composition as a function of sample position, point by point with 0.5 mm steps along x and y axes (around 450 points). The dark sections indicated by "ds" presents the infiltrated region of sample, and the bright sections indicated by "bs" is SiC preform that was not infiltrated by Al_2O_3/Y_2O_3. Fig. 3 (at right) shows the microstructures, obtained by SEM in backscatter mode, of three different points of sample. Micrographs, EDS mapping and microstructural analysis were made for all samples.

Fig. 3(a) indicates the microstructure in the non-infiltrated region where only weakly linked SiC particles are present, i.e., with characteristic structure of preforms. Letter (b) represents the region where the infiltration stopped, composed only of SiC grains and SiC grains surrounded by an intergranular phase. Letter (c) indicates the microstructure in the infiltrated region, composed of SiC grains (dark regions) surrounded by intergranular phase (bright regions). This intergranular phase is the product of Al_2O_3/Y_2O_3 reaction, and it can be $Y_3Al_5O_{12}$ (YAG phase), according phase diagram of Al_2O_3/Y_2O_3 system [21].

The EDS point-mapping shows that the concentrations of Al, Y and O elements decreased severely after 4, 6, 11 and 12 mm in the preforms heated for 5, 10, 30 and 60 min, respectively. Small quantities of Y and O diffused to the non-infiltrated section of the preforms, around 2 wt.%. The Si and C elements were found in all positions, mainly in the section

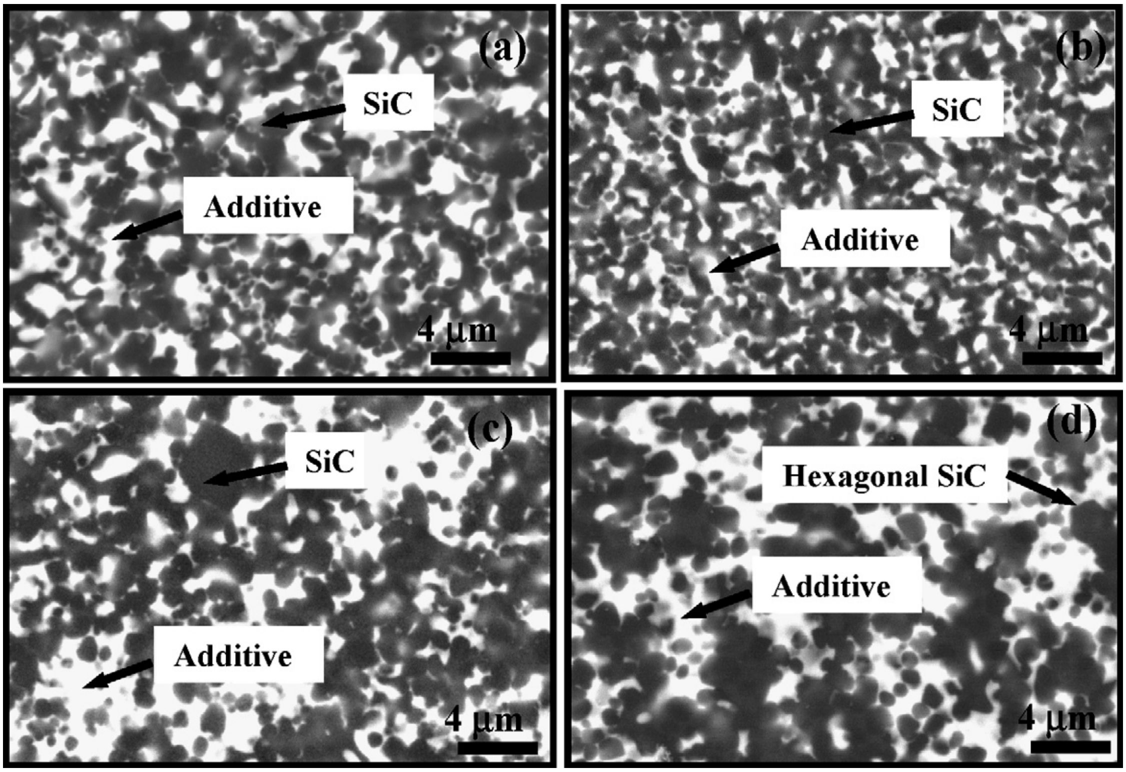

Fig. 4. Microstructures obtained by SEM in backscattering mode of infiltrated preforms at: (a) 5 min, (b) 10 min, (c) 30 min and (d) 60 min.

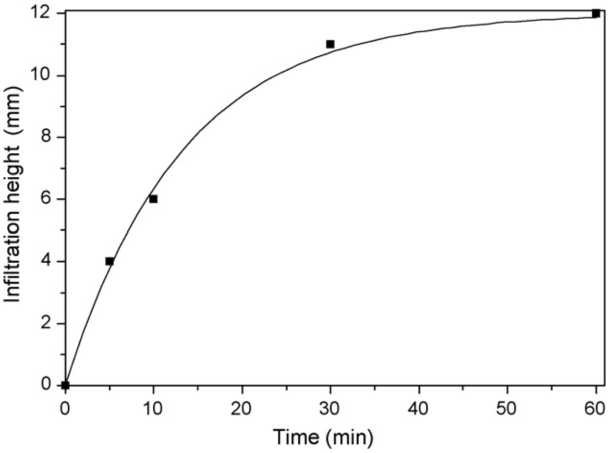

Fig. 5. Infiltration height of Al_2O_3/Y_2O_3 on SiC perform as a function of time.

where Al, Y, and O were not found, as expected. These compositional distributions agree with the difference of sample grayscale shown in Fig. 3 (at left): the dark section indicated by ''ds'' presents Si, C, Al, Y and O, and the bright section indicated by ''bs'' presents Si and C, i.e., the bright section was not infiltrated by the liquid.

Fig. 4 shows the microstructures obtained by SEM in backscatter mode for all infiltrated regions studied. The microstructure of SiC infiltrated by Al_2O_3/Y_2O_3 at 1870 °C for 5 and 10 min presents the characteristic of performs with infiltrated liquid, i.e., no evidence of solution precipitation process, Fig. 4(a and b). In contrast, SiC infiltrated during 30 and 60 min, Fig. 4(c and d) shows some hexagonal SiC grain formation surrounded by Al_2O_3/Y_2O_3, that determine the solution precipitation process, so important to obtain good mechanical properties of SiC ceramics, and growth of SiC grains.

Fig. 5 shows the infiltration height as a function of time of Al_2O_3/Y_2O_3 into SiC preforms. The curve behavior is logarithm, as shown in Eq. (2), where h is the infiltration height (mm) and t is the infiltration time (min). This equation is the formula obtained from mathematical fitting of curve.

$$h = 12(1 - 0.93^t) \tag{2}$$

Initially, the liquid sucked into the preform is accelerated by capillarity. Thereafter, the capillarity is compensated for viscosity so that a quasi-steady state is achieved, and eventually the rise is slowed down by gravity [17]. If infiltration time grows, then the infiltration height tends to 12 mm, even then additional Al_2O_3/Y_2O_3 liquid is able to infiltrate all SiC perform. It means that equilibrium capillary pressure of system is reached in 60 min infiltration. Though the higher infiltration rate occurs before 30 min, the microstructure continues to change, leading to good mechanical properties. It is not necessary to increase the infiltration time beyond 60 min, because no additional infiltration will occur; only microstructure will change and possible reaction between SiC and Al_2O_3/Y_2O_3 will occur, promoting the weight loss during the heat treatment.

Table 1
Vickers hardness (H_v) and fracture toughness (K_{IC}) of SiC infiltrated with Al_2O_3/Y_2O_3 at 1870 °C during 5, 10, 30 and 60 min, in argon atmosphere

Infiltration time (min)	H_v (GPa)	K_{IC} (MPa m$^{1/2}$)
5	21.6 ± 0.7	4.2 ± 0.6
10	20.6 ± 0.6	4.6 ± 0.3
30	20.1 ± 0.2	4.7 ± 0.5
60	21.1 ± 1.0	4.4 ± 0.1

Table 1 shows the Vickers hardness (H_v) and fracture toughness (K_{IC}) of SiC infiltrated with Al_2O_3/Y_2O_3 at 1870 °C for 5, 10, 30 and 60 min, in argon atmosphere. For all infiltration times the hardness is around 20 GPa and the toughness is approximately 4.5 MPa m$^{1/2}$, values of mechanical properties that are comparable to SiC ceramics sintered in presence of Al_2O_3/Y_2O_3 liquid. This indicates that the infiltration process can substitute the conventional process of liquid phase sintering of this system.

4. Conclusions

The unidirectional and spontaneous infiltration process can be used to produce SiC ceramics with properties similar to the SiC ceramics obtained by LPS using Al_2O_3/Y_2O_3 additive.

The SiC grains grow as a function of the infiltration time, and the behavior is similar to LPS, where the ''Ostwald ripping'' phenomenon occurs.

The height of infiltration is not indefinite because it depends on capillarity, but for the studied system the height, h, of the infiltration can be described by an empirical equation of the form $h = 12(1 - 0.93^t)$ where t is the time.

Acknowledgements

The authors are thankful to Fundação de Amparo à Pesquisa do Estado de São Paulo (FAPESP) (Grants 01/10664-6 and 01/11339-1) and Conselho Nacional de Desenvolvimento Científico e Tecnológico (CNPq) (Grants 142090/2001-8 and 302612/2004-1), Brasil, for financial support.

References

[1] P.N. Padture, R.B. Lawn, Toughness properties of a silicon carbide in situ induced heterogeneous grain structure, J. Am. Ceram. Soc. 77 (10) (1994) 2518–2522.
[2] Y.W. Kim, M. Mitomo, H. Emoto, J.G. LEE, Effect of initial α-phase content on microstructure and mechanical properties of sintered silicon carbide, J. Am. Ceram. Soc. 81 (1998) 3136–3140.
[3] V.A. Izhevskyi, L.A. Genova, A.H.A. Bressiani, J.C. Bressiani, Effective sintering aids for silicon carbide ceramics: reactivities of silicon carbide with various additives, Mater. Res. 3 (2000) 131–138.
[4] F.V. Motta, R.M. Balestra, S. Ribeiro, S.P. Taguchi, Wetting behaviour of SiC ceramics: Part I – E_2O_3/Al_2O_3 additive system, Mater. Lett. 58 (2004) 2805–2809.
[5] M.R. Reyes, M.I.P. Canul, E.E.P. Medécigo, A. Gorokhovsky, Effect of Mg loss on the kinetics of pressureless infiltration in the processing of Al–Si–Mg/SiC_p composites, Mater. Lett. 57 (2003) 2081–2089.

[6] K. Konopla, A. Olszówka-Myalska, M. Szafran, Ceramic–metal composites with an interpenetrating network, Mater. Chem. Phys. 81 (2003) 329–332.

[7] N. Frange, N. Levin, M. Gelbstein, M.P. Dariel, Manufacturing B4C-(Al, Si) composite materials by metal alloy infiltration, J. Mater. Process. Technol. 486–490 (2003) 143–144.

[8] Y. Pan, M.X. Gao, F.J. Oliveira, J.M. Vieira, J.L. Baptista, Infiltration of SiC preforms with iron silicide melts: microstructure and properties, Mater. Sci. Eng. A 359 (2003) 343–349.

[9] M.X. Gao, Y. Pan, F.J. Oliveira, J.L. Baptista, J.M. Vieira, Interpenetrating microstructure and fracture mechanism of NiAl/TiC composites by pressureless melt infiltration, Mater. Lett. 58 (2004) 1761–1765.

[10] N.A. Travitztky, E.Y. Gutmanas, N. Claussen, Mechanical properties of Al_2O_3/Si composites fabricated by pressureless infiltration technique, Mater. Lett. 33 (1997) 47–50.

[11] V.M. Kevorkijan, The reactive infiltration of porous ceramic media by molten aluminum alloy, Compos. Sci. Technol. 59 (1999) 683–686.

[12] X.J. Sheng, H. Xu, Z.H. Jin, Y.L. Wang, Preparation of glass-infiltrated 3Y-TZP/Al_2O_3/glass composites, Mater. Lett. 58 (2004) 1750–1753.

[13] A. Mattern, B. Huchler, D. Staudenecker, R. Oberacker, A. Nagel, M.J. Hoffmann, Preparation of interpenetrating ceramic-metal composite, J. Eur. Ceram. Soc. 24 (2004) 3399–3708.

[14] W.C. Tu, F.F. Lange, Liquid precursor infiltration processing of powder compacts 1. Kinetic studies and microstructure development, J. Am. Ceram. Soc. 78 (12) (1995) 3277–3282.

[15] Y. Pan, J.L. Baptista, The infiltration of cobalt silicides into silicon carbide performs, J. Eur. Ceram. Soc. 18 (1998) 201–207.

[16] S.P. Taguchi, F.V. Motta, R.M. Balestra, S. Ribeiro, Wetting behaviour of SiC ceramics: Part II—Y_2O_3/Al_2O_3 and Sm_2O_3/Al_2O_3, Mater. Lett. 58 (2004) 2810–2814.

[17] B.V. Zhmud, F. Tiberg, K. Hallstensson, Dynamics of capillary rise, J. Colloid Interface Sci. 228 (2000) 263–269.

[18] H. Caps, S.J. Cox, H. Decauwer, D. Weaire, N. Vancerwalle, Capillary rise in foams under microgravity, Colloids Surf. A: Physicochem. Eng. Aspects 261 (2005) 131–134.

[19] A. Siebold, M. Nardin, J. Schultz, A. Walliser, M. Oppliger, Effect of dynamic contact angle of capillary rise phenomena, Colloids Surf. A: Physicochem. Eng. Aspects 161 (2000) 81–87.

[20] I.J. McColn, Ceramic Hardness, Plenum Press, New York and London, 1990, p. 324.

[21] T. Noguchi, M. Mizuno, Liquidus curve measurements in the system yttrium oxide-aluminum oxide, Kogyo Kagaku Zassh 70 (6) (1967) 839.